Deletion of K1/K10 does not impair epidermal stratification but affects desmosomal structure and nuclear integrity

Lee Wallace, Leiann Roberts-Thompson and Julia Reichelt*

Institute of Cellular Medicine and North East England Stem Cell Institute, Newcastle University, Framlington Place, Newcastle upon Tyne NE2 4HH, UK

*Author for correspondence (julia.reichelt@ncl.ac.uk)

Accepted 3 December 2011
Journal of Cell Science 125, 1750–1758

doi: 10.1242/jcs.097139

Summary

Keratins K1 and K10 are the most abundant proteins in the upper epidermis where they polymerize to form intermediate filaments (IFs). In addition to their well-established function in providing epidermal stability, K1/K10 (i.e. the dimer between K1 and K10) IFs are supposed to be important for terminal epidermal differentiation and barrier formation. It was previously shown that the imbalanced deletion of one of the partner keratins, K10, disturbed epidermal homoeostasis, although stability was provided by compensatory upregulation of K5/K14, which formed IFs together with the remaining K1. Here, we show that deletion of both partner keratins, K1 and K10, results in lethal postnatal skin fragility in mice. $Krt1^{-/-}$;$Krt10^{-/-}$ mice revealed that K1/K10 IFs are unexpectedly dispensable for epidermal stratification. Although the stratum corneum was less compact and cornified envelope differentiation was impaired, a dye exclusion assay showed that the development of a functional water barrier was surprisingly independent from the presence of K1/K10 IFs. The deletion of K1/K10 was not compensated by any other keratin pair such as the basal epidermal keratins K5/K14, and electron microscopy revealed total absence of IFs in the suprabasal epidermis. Although plakoglobin was unchanged, the expression of the desmosomal proteins desmoplakin, desmocollin 1 and desmoglein 1 were altered and suprabasal desmosomes were smaller in $Krt1^{-/-}$;$Krt10^{-/-}$ than in wild-type epidermis suggesting an involvement of K1/K10 IFs in desmosome dynamics. Furthermore, $Krt1^{-/-}$;$Krt10^{-/-}$ mice showed premature loss of nuclei during epidermal differentiation and lower levels of emerin, lamin A/C and Sun1, revealing a previously unknown function for IFs in maintaining nuclear integrity in the upper epidermis.

Key words: Keratins, Intermediate filaments, Epidermis, Epidermal barrier, Desmosomes, Cell nucleus, Knockout mice

Introduction

Keratins are the major proteins in the epidermis. They build the intermediate filament (IF) cytoskeleton, which provides stability to the tissue (Herrmann et al., 2009). Epidermal IFs are composed of equal amounts of type I (e.g. K10) and type II (e.g. K1) IF proteins. Keratinocytes of the basal epidermal layer express K5, K14 and K15. Upon differentiation, when keratinocytes exit from the basal layer and migrate upwards into the suprabasal layers, these keratins are replaced by K1 and K10. In the specialized thicker epidermis of soles and palms K2 and K9 are additionally expressed to complement the K1/K10 (where K1/K10 indicates the dimer between K1 and K10) = network. In contrast to humans, where K2 is more widely expressed, in mice K2 expression is restricted to foodpad, tail and ear epidermis (Rentrop et al., 1987). Keratins K6, K16 and K17 are normally restricted to hair follicles but upon wound healing and in hyperproliferative conditions their expression is strongly upregulated in the interfollicular epidermis (Kirfel et al., 2003).

Keratin IFs span the cytoplasm and interact with desmosomal cell–cell contacts at the plasma membrane thus integrating neighbouring keratinocytes and ultimately the entire tissue. The interaction between IFs and desmosomes is mediated by binding of keratins to desmoplakin, a member of the plakin family and a major desmosomal component localized to the inner desmosomal plaque (Garrod and Chidgey, 2008). The keratin IF cytoskeleton is also connected to the cell nucleus. This connection is mediated by another plakin family member, the cytoskeletal linker protein plectin, which in turn binds to the outer nuclear membrane protein nesprin-3 (Wilhelmsen et al., 2005). Nesprin-3 binds, through the inner nuclear membrane-spanning SUN proteins, to the nuclear lamina protein lamin A, a type V IF family member and an essential component of the nucleoskeleton (Ketema et al., 2007; Postel et al., 2010; Wilhelmsen et al., 2005). Together, SUN proteins and nesprins constitute the LINC (linker of nucleoskeleton and cytoskeleton) complexes (Crisp et al., 2006). Evidence is emerging that the links between the cytoskeleton and the nuclear lamina play a role in physical signal transduction and gene regulation (Dahl et al., 2008).

Epidermal keratin IFs have a well-established function in providing resilience to the tissue. The specific functions of individual keratins and the significance of the tight local regulation of IF keratin composition during normal epidermal differentiation and disease (Moll et al., 2008) are, however, not well understood. Transgenic mice expressing mutant keratins as well as knockout mice have been generated in the past to address this major question in the keratin field (Magin et al., 2004). Mutant keratins act in a dominant-negative way, being able to integrate into de novo formed or preexisting IFs and thus

impairing their resilience to mechanical load. This results in the collapse of the IF cytoskeleton upon minor mechanical stress, as shown in transgenic mice expressing mutant keratins (Vijayaraj et al., 2007) and in humans with a variety of blistering skin disorders such as epidermolysis bullosa simplex (EBS; mutations in K5 or K14) and epidermolytic ichthyosis (EI; mutations in K1 or K10) (Chamcheu et al., 2011). The study of epidermal keratin mutations underlined their structural importance for tissue stabilization, but keratin mutations are not suitable to study the additional functions of specific keratins and keratin pairs. Deletions of individual keratins in mice have revealed that K14 (Lloyd et al., 1995) and K10 (Reichelt et al., 2001) are partially compensated for by K15 and K14, respectively, whereas lack of K5 is not compensated for by any other keratin, resulting in neonatal lethal epidermolysis (Peters et al., 2001). Absence of K10 is compensated for by subrabasal upregulation of the basal epidermal keratins K5/K14 in *Krt10*$^{-/-}$ mice resulting in suprabasal filament bundles consisting of the remaining partner K1, K5 and K14 (Reichelt et al., 2001). K1/K5/K14 IFs have similar properties as K1/K10 IFs with respect to their ability to provide stability to the suprabasal epidermis and resilience to mechanical load, however, the imbalanced keratin expression impairs epidermal homoeostasis causing hyperproliferation, increased epidermal turnover and epidermal thickening including hyperkeratosis (Reichelt and Magin, 2002). Although single keratins have been deleted in mice, an entire epidermal keratin expression pair has not yet been deleted.

Besides their well-established role in providing epidermal stability, K1/K10 filaments are believed to be important for epidermal barrier formation because they are highly crosslinked with the cornified envelope (Candi et al., 2005). Upon terminal differentiation in the granular layer of the upper epidermis, the precursor protein profilaggrin is processed to filaggrin, which interacts with keratin IFs and aggregates them into tight bundles oriented parallel to the epidermal surface (Gan et al., 1990). This process is thought to be responsible for the flattening of keratinocytes that occurs during the transition from spinous to granular layer. Together keratins and filaggrin constitute >80% of the protein mass of the epidermis, so it was proposed that this is important to provide a scaffold for the assembly of a variety of differentiation-specific proteins such as involucrin and loricrin, which are crosslinked by transglutaminases to form the cornified envelope. The cornified envelope replaces the cell membrane during terminal differentiation and forms, together with the

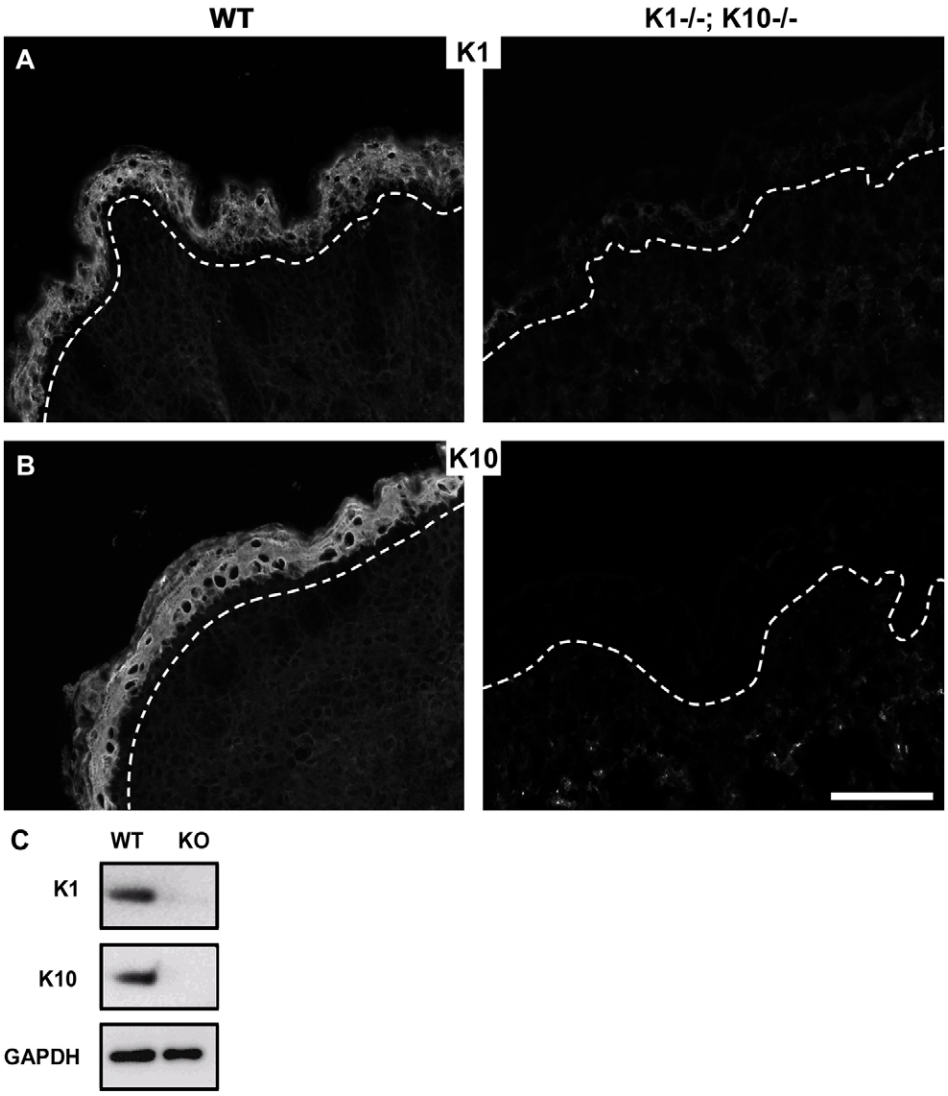

Fig. 1. Expression of K1 and K10 in mouse skin. (**A**,**B**) Immunofluorescence analysis showing suprabasal expression of K1 and K10 in wild-type skin and absence of both keratins in *Krt1*$^{-/-}$;*Krt10*$^{-/-}$ (K1$^{-/-}$/K10$^{-/-}$) mice. (**C**) Western blotting confirming the absence of K1 and K10 protein in *Krt1*$^{-/-}$;*Krt10*$^{-/-}$ skin. GAPDH was used as loading control. WT, wild type; KO, *Krt1*$^{-/-}$;*Krt10*$^{-/-}$. Dashed lines indicate basement membrane. Scale bar: 100 μm.

attached lipid envelope, the epidermal barrier (Candi et al., 2005).

We generated *Krt1*$^{-/-}$;*Krt10*$^{-/-}$ mice in order to study whether this keratin pair is essential for the upper epidermis, for epidermal differentiation, including cornified envelope assembly, or whether K1/K10 might be replaced by balanced suprabasal K5/K14 expression. We describe the consequences of total absence of IFs in the suprabasal layers of the epidermis resulting from K1/K10 deletion in mice, leading to lethal postnatal skin fragility. Our data demonstrate that K1/K10 IFs are, in contrast to what was previously believed, dispensable for epidermal stratification and formation of a functional water barrier. Furthermore, our results indicate that K1/K10 IFs are integral to the dynamic structure of desmosomes, and most importantly point to a previously unknown and essential function for IFs in the maintenance of nuclear integrity.

Results

Krt1$^{-/-}$;*Krt10*$^{-/-}$ mice were derived from single, K1 (T. Magin and J.R., unpublished) and K10 (Reichelt et al., 2001) keratin knockout mice by breeding over two generations. Double heterozygous, *Krt1*$^{+/-}$;*Krt10*$^{+/-}$, mice from the F1 generation were normal and were used for further breeding. F2 generation pups from matings of double heterozygous parents (*Krt1*$^{+/-}$;*Krt10*$^{+/-}$) were born at the expected Mendelian ratio with 1/16 *Krt1*$^{-/-}$;*Krt10*$^{-/-}$ pups. Complete absence of both K1 and K10 protein from *Krt1*$^{-/-}$;*Krt10*$^{-/-}$ skin was confirmed by immunofluorescence analysis of skin sections and western blotting (Fig. 1). Initially, the skin of all neonates appeared indistinguishable. However, the epidermis of *Krt1*$^{-/-}$;*Krt10*$^{-/-}$, as well as *Krt1*$^{+/-}$;*Krt10*$^{-/-}$ and *Krt1*$^{-/-}$;*Krt10*$^{+/-}$ mice was fragile upon mechanical load giving rise to generalized multiple small and some extended lesions particularly on the palms (Fig. 2E,F), resulting in death within the first hours after birth. Surprisingly, using a dye-exclusion assay on embryonic day (E) 18.5 embryos, we found that the water barrier of *Krt1*$^{-/-}$;*Krt10*$^{-/-}$, as well as *Krt1*$^{+/-}$;*Krt10*$^{-/-}$ and *Krt1*$^{-/-}$;*Krt10*$^{+/-}$ mice, was, as in wild-type controls, fully developed before birth, and the dye was only able to penetrate the epidermis at lesional sites (Fig. 2A–D). These results showed that K1/K10 filaments are essential for epidermal stability but dispensable for the development of a functional epidermal water barrier.

In order to establish whether cornified envelopes were formed normally in the absence of K1/K10, we isolated cornified envelopes from neonatal mouse skin. Although a substantial proportion of isolated cornified envelopes from *Krt1*$^{-/-}$;*Krt10*$^{-/-}$ skin (Fig. 2H, arrowheads) looked similar to those of wild-type skin (Fig. 2G), almost 40% were misshapen (n=911). Some of these misshapen cornified envelopes showed inclusions (Fig. 2H, arrow), others appeared empty (Fig. 2H, asterisks). During microscopic analysis of freshly prepared samples we observed that inclusion-containing cornified envelopes ruptured upon

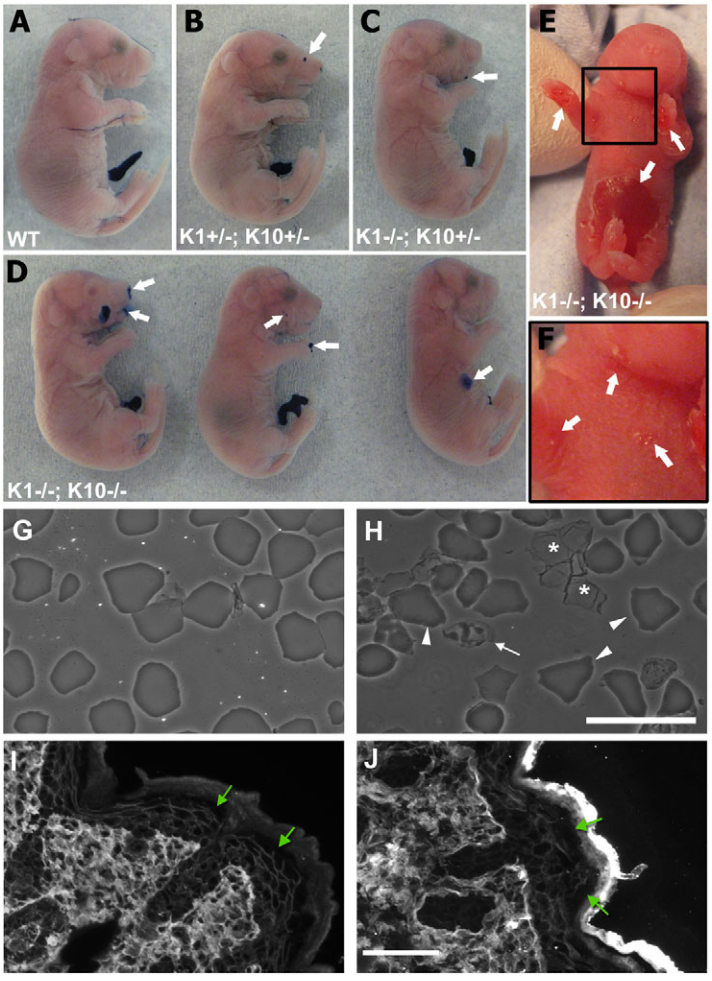

Fig. 2. Analysis of the epidermal barrier function. (**A–D**) The dye exclusion assay showed that *Krt1*$^{-/-}$;*Krt10*$^{-/-}$ (D), like wild-type skin (A), had developed an intact water barrier by E18.5. Note the intense staining of the umbilical cord, which serves as positive internal control for a missing barrier. Stained patches (arrows) on *Krt1*$^{-/-}$;*Krt10*$^{-/-}$ skin (D) and *Krt1*$^{+/-}$;*Krt10*$^{-/-}$ (B) and *Krt1*$^{-/-}$;*Krt10*$^{+/-}$ (C) indicate lesions induced by sample preparation. (**E**,**F**) During the first hours after birth *Krt1*$^{-/-}$;*Krt10*$^{-/-}$ mice developed many large (E, arrows) and minute skin lesions (F, arrows; higher magnification of framed area in E). (**G**,**H**) The majority of isolated cornified envelopes from *Krt1*$^{-/-}$;*Krt10*$^{-/-}$ skin (H, arrowheads) were similar to those of wild-type skin (G), however, some cornified envelopes showed inclusions (H, arrow) and others appeared as empty shells (H, asterisks). (**I**,**J**) The permeability assay showed that subepidermally injected biotin, visualised by using streptavidin–Alexa-Fluor-594 on skin sections, entered the intercellular spaces of the epidermis in wild-type (I) and *Krt1*$^{-/-}$;*Krt10*$^{-/-}$ (J) skin, but was unable to pass the upper stratum granulosum, leaving an unstained gap between the living layers and the stratum corneum (arrows). Note a strong background staining in the stratum corneum in *Krt1*$^{-/-}$;*Krt10*$^{-/-}$ skin. Scale bars: 50 μm.

mechanical load and released their contents, leaving empty shells. Our findings suggest that although cornified envelopes are formed in the absence of IFs, they are less robust.

Transepidermal water loss (TEWL) measurements to identify inside-out barrier defects were not performed because of the large amount of micro-lesions present in *Krt1*$^{-/-}$;*Krt10*$^{-/-}$ epidermis, which would result in artificially increased TEWL measurements (Leclerc et al., 2009). Instead, we used a permeability assay, allowing assessment of tight junction function in the upper epidermis (Furuse et al., 2002), to test the inside-out barrier. The subepidermally injected tracer (560 Da) entered the intercellular spaces of the epidermis, but was unable to pass beyond the level of the upper stratum granulosum in both wild-type (Fig. 2I, arrows) and *Krt1*$^{-/-}$;*Krt10*$^{-/-}$ skin (Fig. 2J, arrows). This result showed that establishment of the tight junction-dependent epidermal barrier in the granular layer is independent from the presence of K1/K10 IFs.

Ultrastructural comparison of *Krt1*$^{-/-}$;*Krt10*$^{-/-}$ and wild-type skin (both E18.5) revealed that the suprabasal layers of *Krt1*$^{-/-}$;*Krt10*$^{-/-}$ epidermis were completely devoid of IFs (Fig. 3A,B). Desmosomes were localized normally at the cell membranes and the distribution of keratohyalin granules was normal in the granular layers but suprabasal keratinocytes were less flattened in *Krt1*$^{-/-}$;*Krt10*$^{-/-}$ epidermis than in wild-type controls (Fig. 3A–D). Although the *Krt1*$^{-/-}$;*Krt10*$^{-/-}$ mice had a functional water barrier, transmission electron microscopy (TEM) analysis revealed that the stratum corneum was less compact than in wild-type skin, looking thicker and disorganized (Fig. 3E,F), consistent with the impairment of cornified envelope differentiation.

Previous studies on *Krt10*$^{-/-}$ mice showed that deletion of one suprabasal keratin can be compensated for by upregulation of basal keratins (Reichelt et al., 2001). Although protein levels of the basal keratins K5 and K14, as well as the wound healing-associated keratin K6, were higher in *Krt1*$^{-/-}$;*Krt10*$^{-/-}$ skin, as shown by western blotting (Fig. 4G), immunofluorescence analysis of skin sections revealed that K5 and K14 remained restricted to the basal epidermal layer (Fig. 4A,B), and K6 to hair follicles (Fig. 4C). We noted strong K6 staining of the stratum corneum in *Krt1*$^{-/-}$;*Krt10*$^{-/-}$ skin, which might be either background resulting from unspecific antibody binding to the loose stratum corneum, or indeed reflect the higher levels of K6 detected by western blotting. Monomeric K6 might be undetectable or washed out from the living epidermal layers during processing of the sections but be detectable again in the stratum corneum because of crosslinking to the cornified envelope scaffold. We also checked for expression levels of K2, normally restricted to specific skin regions such as palm and sole epidermis (Rentrop et al., 1987), and for K15, and found that neither of these keratins was upregulated in *Krt1*$^{-/-}$;*Krt10*$^{-/-}$ back skin epidermis (Fig. 4G) and that their epidermal expression patterns were the same as in the wild type (from immunofluorescence analysis; data not shown).

The keratinocyte differentiation programme seemed to be normal in *Krt1*$^{-/-}$;*Krt10*$^{-/-}$ epidermis, and differentiation markers filaggrin, involucrin and loricrin were expressed in the same layers as in the wild type (Fig. 4D–F). The assessment of suprabasal immunostainings was difficult in *Krt1*$^{-/-}$;*Krt10*$^{-/-}$ cryosections because of the ubiquitous cytolytic tissue damage (Fig. 4D right, asterisks), most probably induced by sample handling and processing. Western blotting showed that the

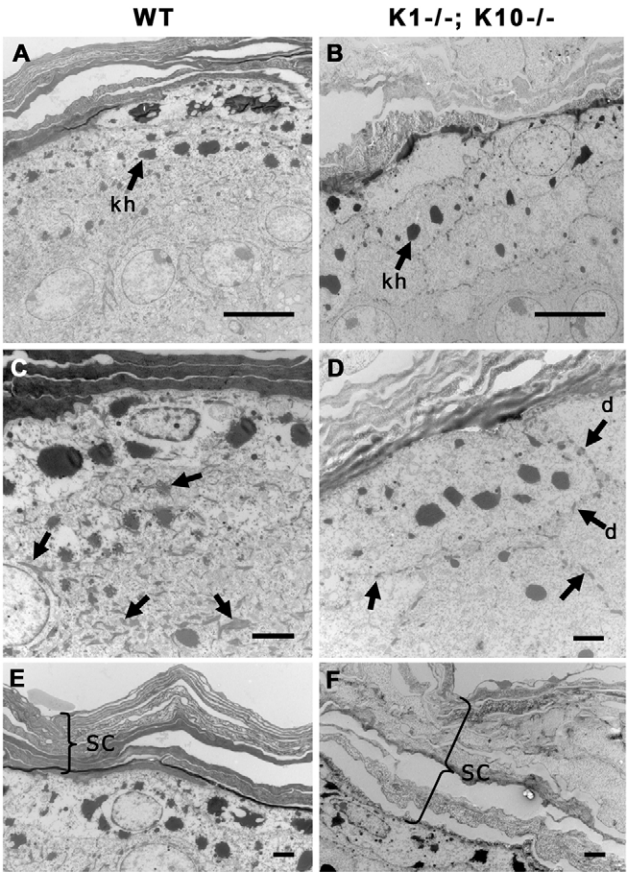

Fig. 3. Ultrastructural analysis of the epidermis. (**A–D**) TEM analysis of epidermis showed that suprabasal keratinocytes were devoid of IFs and had a clear cytoplasm in *Krt1*$^{-/-}$;*Krt10*$^{-/-}$ epidermis (B), whereas IFs bundles were ubiquitously present and prominent in wild-type mice (A,C, arrows). Keratohyalin (kh) granules were abundant in both wild-type and *Krt1*$^{-/-}$;*Krt10*$^{-/-}$ epidermis (A,B, arrows). Note that in the absence of cytoplasmic IFs, cell boundaries, outlined by desmosomes (D, arrows, d), are more visible in *Krt1*$^{-/-}$;*Krt10*$^{-/-}$ than in the wild-type epidermis. (**E**,**F**) The stratum corneum (SC) was less compact in *Krt1*$^{-/-}$;*Krt10*$^{-/-}$ (F) than in wild-type (E) skin. Scale bars: 10 μm (A,B), 2 μm (C–F).

amounts of profilaggrin and involucrin were higher in *Krt1*$^{-/-}$;*Krt10*$^{-/-}$ skin lysates whereas loricrin was much lower (Fig. 4G). Although, the higher amount of profilaggrin in *Krt1*$^{-/-}$;*Krt10*$^{-/-}$ skin was processed normally through the same intermediates to filaggrin monomers as in the wild type, the level of mature filaggrin was not greater, as assessed by western blotting (Fig. 4G). This result shows that proteolytic maturation of profilaggrin to filaggrin does not involve regulation by K1/K10 filaments, and suggests that lack of IFs in the upper epidermis of *Krt1*$^{-/-}$;*Krt10*$^{-/-}$ mice, and thus failure of IFs–filaggrin bundling, destabilizes filaggrin, resulting in accelerated further breakdown into free amino acids. Owing to the mixed mouse strain background in the F2 generation of analyzed mice, we found different involucrin alleles expressed (Fig. 4G). The sizes of the detected polypeptides corresponded to the previously published sizes for involucrin in BALB/c mice: 95 kDa, and C57BL/6 mice: 100 kDa (Reichelt et al., 1999).

Our data demonstrate that the observed fragility of *Krt1*$^{-/-}$;*Krt10*$^{-/-}$ epidermis was due to the lack of compensation

by another keratin pair such as K5/K14, and the resulting total absence of suprabasal IFs. The results further support the assumption that filaggrin-mediated parallel aggregation of IFs is essential for keratinocyte flattening and compaction during terminal differentiation.

Ultrastructural analysis of E18.5 skin revealed smaller desmosomes in *Krt1*$^{-/-}$;*Krt10*$^{-/-}$ (194±94 nm, n=200) compared with wild-type upper epidermis (306±155 nm, n=111; with P<0.001), and absence of the midline (Fig. 5A, arrows). The smaller desmosomes and structural abnormality were in line with weaker membrane immunostainings for desmoplakin (Fig. 5B) and desmocollin (Fig. 5C) in *Krt1*$^{-/-}$;*Krt10*$^{-/-}$ skin sections compared with wild-type skin. Western blotting showed that the overall amount of desmoplakin in total protein skin lysates was slightly higher whereas desmocollin 1 and desmoglein 1 were lower in *Krt1*$^{-/-}$;*Krt10*$^{-/-}$ compared with the wild type (Fig. 5G). Plakoglobin was found, by immunostaining and western blotting, to be unaltered (Fig. 5F,G). The adherens junction proteins E-cadherin and β-catenin were both localized to the cell membranes (Fig. 5D,E). Although β-catenin protein levels were unaltered, both E-cadherin and actin were lower in *Krt1*$^{-/-}$;*Krt10*$^{-/-}$ skin lysates (Fig. 5G). Both desmocollin and E-cadherin stainings showed strong background in the stratum corneum.

Our results show that K1/10 filaments are important for the integrity of desmosomes and adherens junctions in the suprabasal epidermis.

TEM analysis, as well as DAPI staining of cryosections of E18.5 skin, indicated a premature degradation of nuclei in *Krt1*$^{-/-}$;*Krt10*$^{-/-}$ suprabasal epidermis (Fig. 6A,B). K1/K10 deletion did not affect proliferation, which remained restricted to the basal layer, as demonstrated by Ki-67 staining (Fig. 6C). In line with the fewer suprabasal nuclei, immunolabelling of the nuclear lamina proteins emerin (Fig. 6D) and lamin A/C (Fig. 6E) was strongly reduced. Western blotting confirmed these results and also revealed diminished levels of Sun1 (Fig. 6F).

The premature loss of nuclei in *Krt1*$^{-/-}$;*Krt10*$^{-/-}$ epidermis points to a function of K1/K10 filaments in the maintenance of nuclear integrity and/or orderly nuclear degradation during terminal differentiation.

Discussion

Loss of K1/K10 is not compensated by the basal keratin pair K5/K14

The lack of compensation of K1/K10 deletion by endogenous K5/K14 was unexpected because previous data from *Krt10*$^{-/-}$ mice showed suprabasal K5/K14 stabilization. In light of our findings, K5/K14 stabilization in *Krt10*$^{-/-}$ mice was probably due to the

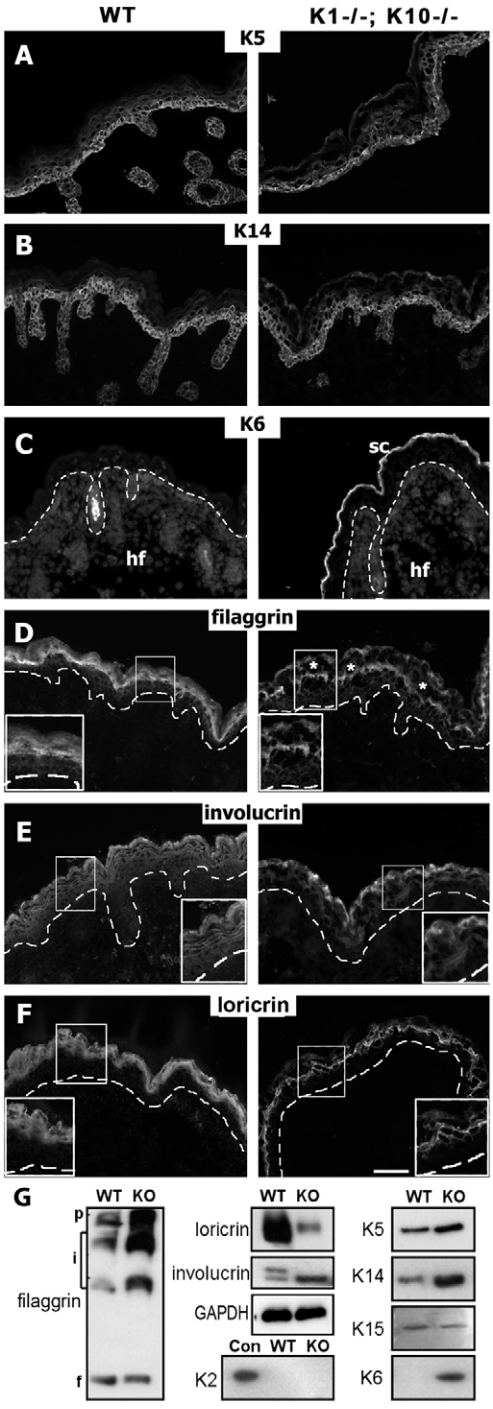

Fig. 4. Analysis of the epidermal differentiation programme. (**A–C**) Immunofluorescence analysis revealed that IFs containing K5 (A) and K14 (B) remained restricted to the basal epidermal layer, and IFs containing K6 (C) remained restricted to hair follicles in *Krt1*$^{-/-}$;*Krt10*$^{-/-}$ skin. (**D–F**) The differentiation markers filaggrin, involucrin and loricrin were detected in the suprabasal layers in *Krt1*$^{-/-}$;*Krt10*$^{-/-}$ epidermis on skin sections (insets show higher magnification of framed areas). Note that all cryosections from *Krt1*$^{-/-}$;*Krt10*$^{-/-}$ skin showed cytolysis in the upper suprabasal epidermal layers (D, asterisks), and anti-K6 antibodies showed a strong, possibly background staining in the stratum corneum (C, sc). Hf, hair follicle. Dashed lines indicate basement membrane. (**G**) Western blotting revealed that expression of K5, K14 and K6 was higher in *Krt1*$^{-/-}$;*Krt10*$^{-/-}$ skin extracts, in contrast to K15, which was unaltered. Although, deduced from immunofluorescence analysis, their expression seemed to be lower compared with the wild type. Only loricrin expression was much lower, whereas both involucrin and profilaggrin were higher. Although profilaggrin and the processed intermediates were higher, the amount of mature filaggrin was unaltered. Note that different sized bands for involucrin resulted from different mouse strain-specific alleles (Reichelt et al., 1999). K2, which is normally expressed in sole epidermis but not in trunk skin, was not induced in *Krt1*$^{-/-}$;*Krt10*$^{-/-}$ back skin. Con, control protein lysate from wild-type paw skin; p, profilaggrin; i, intermediate stages of profilaggrin processing; f, filaggrin; WT, wild type; KO, *Krt1*$^{-/-}$;*Krt10*$^{-/-}$. GAPDH was used as loading control. Scale bar: 100 μm.

continued presence of K1. In previous transfection studies in cell culture (Kartasova et al., 1993) and in vivo in *Krt5*$^{-/-}$ and *Krt10*$^{-/-}$ mice, K1 was shown to be able to form filaments with K14 (Peters et al., 2001; Reichelt et al., 2001) and integrate into K5/K14 filaments (Reichelt et al., 2001). Our findings suggest that K5/K14 IFs are not stable in suprabasal layers without K1.

The total absence of IFs in the upper suprabasal epidermis of *Krt1*$^{-/-}$;*Krt10*$^{-/-}$ mice caused cell and tissue fragility resulting in fatal skin lesions in neonatal mice, furthermore underlining the structural importance of epidermal keratin IFs for tissue stability. In line with our results is the fragility of the basal epidermal layer and extensive blister formation in *Krt5*$^{-/-}$ mice (Peters et al., 2001). Because of the lack of compensation by another type II keratin, K5 deletion results in almost complete absence of IFs in the basal epidermis. In contrast to the situation in the upper suprabasal layers of *Krt1*$^{-/-}$;*Krt10*$^{-/-}$ mice, which were completely devoid of IFs, in *Krt5*$^{-/-}$ mice the remaining basal keratin partner, K14, was able to form some filaments with K1 in a couple of basal keratinocytes and also in the lower suprabasal (spinous) layers, possibly supporting assembly of the suprabasal K1/K10 cytoskeleton in *Krt5*$^{-/-}$ mice (Kartasova et al., 1993).

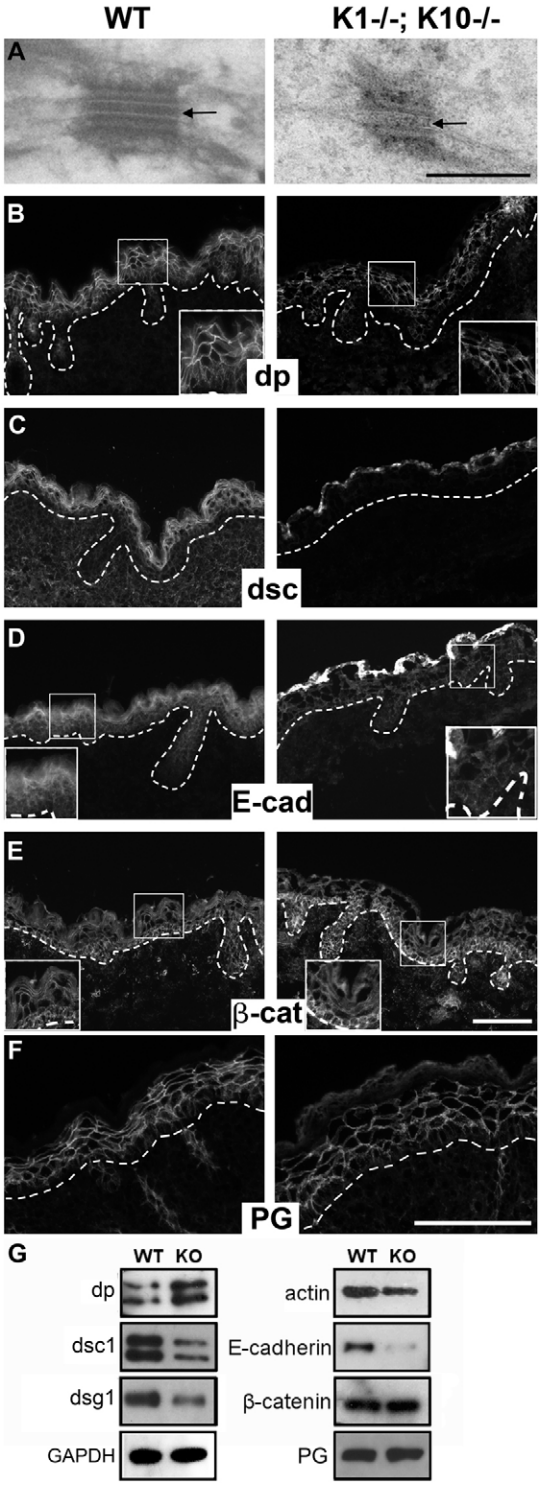

Absence of K1/K10 IFs does not impair stratification and barrier formation

Together, both keratin knockout mouse models, *Krt1*$^{-/-}$;*Krt10*$^{-/-}$ and *Krt5*$^{-/-}$, clearly demonstrate that keratins do not determine the overall epidermal differentiation programme. It was not surprising that *Krt5*$^{-/-}$ mice developed an intact epidermal barrier because suprabasal differentiation, including expression of K1/K10 was normal in those mice (Peters et al., 2001). However, formation of a functional barrier in *Krt1*$^{-/-}$;*Krt10*$^{-/-}$ mice was surprising as K1/K10 IFs are among the first proteins to be crosslinked during the cornification process to provide a scaffold for other cornified envelope proteins, and were therefore thought to play an important role in barrier maturation and reinforcement (Candi et al., 2005). The observed increased cornified envelope fragility in *Krt1*$^{-/-}$;*Krt10*$^{-/-}$ mice confirmed this. Involucrin and filaggrin, both also early components in cornified envelope assembly, are both higher in *Krt1*$^{-/-}$;*Krt10*$^{-/-}$ skin and possibly partially compensate for the lack of IFs in the cornified envelopes of *Krt1*$^{-/-}$;*Krt10*$^{-/-}$ mice. Loricrin is the most abundant protein of the cornified envelope (>70%). It is normally crosslinked to keratin and filaggrin, which is supposed to support cell flattening (Candi et al., 2005). The reduction in loricrin and the lack of filaggrin–keratin IF bundles in *Krt1*$^{-/-}$;*Krt10*$^{-/-}$ might contribute to the reduced flattening of keratinocytes in *Krt1*$^{-/-}$;*Krt10*$^{-/-}$ skin. Combined with the smaller desmosomes, which normally, after profound morphological changes, also become integrated at an early stage into the cornified envelope, this might contribute to the reduced compaction of the stratum corneum in *Krt1*$^{-/-}$;*Krt10*$^{-/-}$ mice.

Fig. 5. Analysis of desmosomes and adherens junctions. (**A**) TEM analysis revealed that desmosomes in the suprabasal layers were smaller in *Krt1*$^{-/-}$;*Krt10*$^{-/-}$ than in wild-type epidermis and that the midline was absent in *Krt1*$^{-/-}$;*Krt10*$^{-/-}$ (arrows). (**B–F**) Immunofluorescence analysis showed weaker membrane stainings of desmoplakin (dp, B) and desmocollin (dsc, C) in *Krt1*$^{-/-}$;*Krt10*$^{-/-}$ epidermis compared with the control. E-cadherin was also lower in *Krt1*$^{-/-}$;*Krt10*$^{-/-}$ epidermis compared with wild-type controls (D). Expression of β-catenin (E) and plakoglobin (PG, F) were unaltered. (**G**) Western blotting, however, revealed higher levels of desmoplakin in *Krt1*$^{-/-}$;*Krt10*$^{-/-}$ compared with wild-type skin protein extracts and confirmed lower desmocollin 1, desmoglein 1 and E-cadherin expression, and unaltered levels of β-catenin and plakoglobin. Insets in B, D and E show higher magnifications of framed areas. Note strong, possibly background staining for anti-desmocollin and anti-E-cadherin antibodies in the stratum corneum (C,D). (**G**) Western blots revealed lower actin expression in skin extracts from *Krt1*$^{-/-}$;*Krt10*$^{-/-}$. GAPDH was used as loading control. WT, wild type; KO, *Krt1*$^{-/-}$;*Krt10*$^{-/-}$. Dashed lines indicate basement membranes. Scale bars: 0.5 μm (A), 100 μm (E,B–D,F).

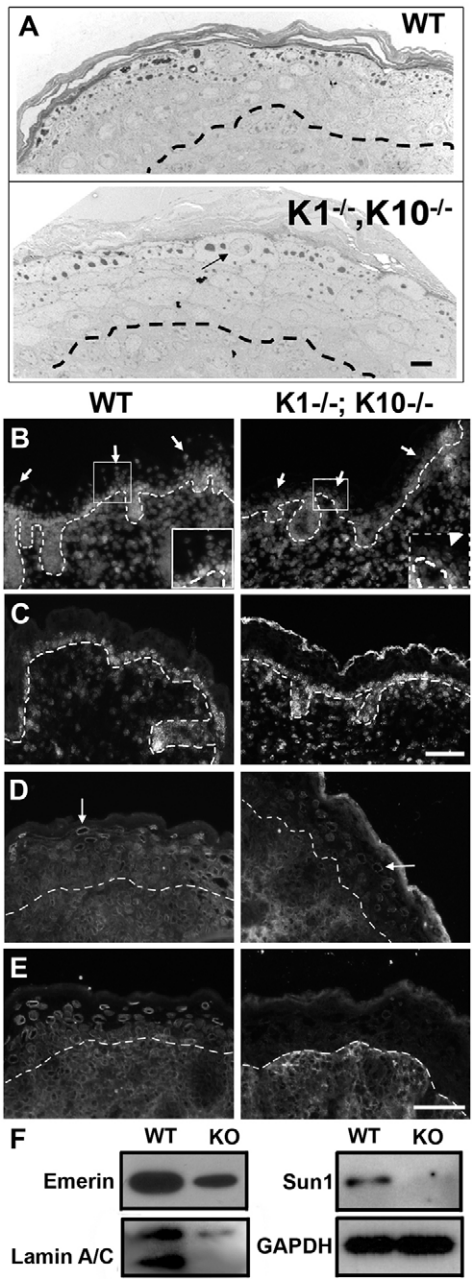

Fig. 6. Analysis of epidermal nuclei. (**A**) TEM revealed less flattening of suprabasal keratinocytes and fewer nuclei, with very rare large, round nuclei (arrow) in the granular layer in *Krt1*$^{-/-}$;*Krt10*$^{-/-}$ epidermis compared with wild-type epidermis (E18.5). (**B**) The fewer nuclei in the upper epidermis was confirmed by DAPI staining (arrows; insets show higher magnification of framed areas). (**C**) Cell proliferation, as revealed by Ki-67 immunostaining, was unaltered. (**D**,**E**) Immunofluorescence analysis showed that emerin (D) and lamin A/C (E) were strongly reduced in *Krt1*$^{-/-}$;*Krt10*$^{-/-}$ epidermis compared with the wild type. (**F**) Lower levels of emerin and lamin A/C were confirmed by western blotting, which also revealed a reduction in Sun1. GAPDH was used as loading control. WT, wild type; KO, *Krt1*$^{-/-}$;*Krt10*$^{-/-}$. Dashed lines indicate basement membranes; arrows in D point to individual nuclei. Scale bars: 10 μm (A), 100 μm (C,B), 50 μm (E,D).

There have been reports of strong redundancy among cornified envelope proteins (Sevilla et al., 2007), and loricrin-deficient mice only display a mild phenotype (Koch et al., 2000).

Desmosomes are smaller in the absence of K1/K10 IFs

Desmosomes are dynamic cell–cell contact structures that anchor IFs to the cytoplasmic membrane. In simple epithelia desmosomes are able to exist independently from IFs, as shown by the presence of normal desmosomes in hepatocytes of mice that lack K8/K18 (Magin et al., 1998). Upon deletion of the simple epithelial keratin K8 in embryonic stem (ES) cells, its partners K18 and K19 were unable to form filaments (Baribault and Oshima, 1991). The absence of IFs did not, however, impair desmosome formation in embryoid bodies after ES cell differentiation. Furthermore, total absence of IFs in the basal epidermal layer in K5-deficient mice (Peters et al., 2001) as well as in epidermolysis bullosa simplex patients bearing a premature termination codon in K14, resulting in a human K14 knockout, did not interfere with normal desmosome or hemidesmosome formation (Chan et al., 1994). Although desmosomes could form in the absence of IFs, desmosome dynamics are modulated by interaction with IFs. Using SCC-9 and A431 cell lines, both originating from stratifying epithelia, another study showed that not only do cell–cell interactions and actin filaments influence desmoplakin dynamics but that deletion of the C-terminal IF-binding domain of desmoplakin, which abolishes keratin binding to desmosomes, impairs desmoplakin dynamics, which are considered important for desmosome assembly and maturation during epithelial remodeling (Godsel et al., 2005). Our data revealed smaller desmosomes and altered expression of desmosomal proteins in the upper epidermis of *Krt1*$^{-/-}$;*Krt10*$^{-/-}$ mice, suggesting that the impact of IFs on desmosome structure depends on the tissue context, the differentiation state and possibly the keratin composition of IFs.

Transfection studies showed that filaggrin might alter the normal distribution of desmosomal proteins, resulting in cytoplasmic accumulation of desmoplakin and also, independently from the presence of IFs, cause disruption of actin filaments (Presland et al., 2001). The increase in unbound filaggrin might thus contribute to the observed decrease in actin and the alterations in desmoplakin localization in *Krt1*$^{-/-}$;*Krt10*$^{-/-}$ epidermis. The interdependence of desmosomes and adherens junctions in the epidermis was highlighted by the conditional knockout of desmoplakin in the epidermis, which resulted in the absence of adherens junctions (Vasioukhin et al., 2001). The lower expression of E-cadherin in *Krt1*$^{-/-}$;*Krt10*$^{-/-}$ epidermis might therefore be a consequence of the alterations in desmosomal organization.

Lack of suprabasal IFs causes premature loss of nuclei during epidermal differentiation

Despite the premature loss of nuclei in the suprabasal epidermis, the overall epidermal differentiation programme was essentially normal in *Krt1*$^{-/-}$;*Krt10*$^{-/-}$ mice, suggesting that nuclear loss is not due to accelerated differentiation but to a specific dependence of nuclear integrity on the presence of K1/K10 IFs. The IF cytoskeleton is connected to the nucleoskeleton by plectin and a LINC complex consisting of nesprin-3 and SUN proteins that bridges the nuclear envelope and binds to lamin A in the nuclear lamina (Wilhelmsen et al., 2005). Deletion of nesprin-3 in zebrafish resulted in a reduction of IFs around the nucleus (Postel et al., 2010), and knockdown of nesprin-2 in HaCaT cells resulted in the absence of perinulear IFs and reduced DAPI staining (Schneider et al., 2011). These results show that deletion of one of the linker molecules can cause decoupling of the IF cytoskeleton from the nucleus. However, deletion of the IF

network can also affect the nucleus. Ablation of desmin, a type III IF protein, which homopolymerizes to form the IF cytoskeleton in myocytes, resulted in nuclear mispositioning in mice (Milner et al., 1996), similar to the situation in muscles lacking lamin A (Mejat et al., 2009). Mechanical coupling between the cell membrane, the cytoplasm and the nucleus has been well documented and it emerged in recent years that direct transduction of mechanical forces through the cytoskeleton to the nucleoskeleton is also involved in gene regulation (Dahl and Kalinowski, 2011; Razafsky and Hodzic, 2009). Lamin A and several inner nuclear membrane proteins, such as MAN1, are known to associate with gene regulatory proteins (Stewart et al., 2007). Although the exact mechanism is still unclear, MAN1 interacts with R-Smads, attenuating TGF-β signalling (Lin et al., 2005).

In the epidermis, keratin IFs are the major cytoskeletal filaments, and the observed premature nuclear loss in *Krt1*$^{-/-}$;*Krt10*$^{-/-}$ epidermis might be connected to the decoupling of the nucleoskeleton from the IF cytoskeleton.

Krt1$^{-/-}$;*Krt10*$^{-/-}$ mice represent the first double knockout mouse model of an epidermal keratin expression pair. Here, we describe the consequences of K1/K10 deletion for epidermal stability and terminal differentiation, and identify unexpected functions for K1/K10 IFs in maintaining desmosomal and nuclear integrity, with possibly broader implications for IFs in general.

Materials and Methods

Generation of K1/K10 double knockout mice

Krt1$^{-/-}$;*Krt10*$^{-/-}$ mice were derived from single K1 and K10 knockout mice (T. Magin and J.R., unpublished) (Reichelt et al., 2001) by breeding over two generations. Double heterozygous *Krt1*$^{-/-}$;*Krt1*$^{+/-}$ mice resulting from the first crossing (F1) were then further bred to obtain double knockout *Krt1*$^{-/-}$;*Krt10*$^{-/-}$ mice in the next generation (F2). *Krt1*$^{+/-}$ mice, used for initial breeding, were on a C57BL/6 strain background (kindly provided by Thomas Magin, University of Leipzig, Germany), whereas *Krt10*$^{-/-}$ mice were on a BALB/c background. *Krt1*/*Krt10* genotypes were determined by polymerase chain reaction using the Phire Animal Tissue Direct PCR kit (Finnzymes, Espoo, Finland).

For analyses, samples from *Krt1*$^{-/-}$;*Krt10*$^{-/-}$ mice were compared with wild-type (*Krt1*$^{+/+}$;*Krt10*$^{+/+}$) control samples from either the same or other litters.

Animals were humanely killed in accordance with the UK Animals Scientific Procedures Act, 1986. All procedures were also approved by the Newcastle University animal ethics committee.

Immunofluorescence analysis

Cryosections (5 μm) of neonatal and E18.5 skin were fixed for 10 minutes with pre-cooled acetone at –20℃. Immunofluorescence analysis was performed as previously described (Reichelt et al., 1997). Antibodies were diluted as follows: anti-K1 (NCL-CK1, Leica, Milton Keynes, UK), 1:250; anti-K10 (DE-K10, Progen, Heidelberg, Germany), 1:10; anti-K5 (Covance, Berkeley, CA), 1:1000; anti-K14 (GPCK14.2, Progen), 1:100; anti-K6 (Ks6.Ka12, Progen), 1:10; anti-filaggrin (PRB-417P, Covance), 1:1000; anti-involucrin (PRB-140C, Covance), 1:1000; anti-loricrin (PRB-145P, Covance), 1:1000; anti-desmoplakin (DP1&2-2.15, Progen), 1:10; desmocollin (52-3D, David Garrod, Manchester University, UK), undiluted; E-cadherin (4065, NEB, Hitchin, UK), 1:20; β-catenin (Millipore, Watford, UK), 1:250; anti-Ki-67 (Dianova, Hamburg, Germany), 1:50; anti-emerin (4G5, Abcam, Cambridge, UK), 1:20; anti-lamin A/C (4C11, Cell Signaling; NEB), 1:20; anti-Sun1 (282, a kind gift from Akis Karakesisoglou, Durham University, UK), 1:20.

Nuclei were stained with DAPI (Invitrogen, Paisley, UK) and secondary antibodies were species-specific Cy3-, Cy2-, Alexa-Fluor-594- or Alexa-Fluor-488-conjugated goat antibodies (Molecular Probes, Eugene, OR). Microscopical analyses were performed using an Axio Imager Z2 operated through Axiovision software (Zeiss, Hertfordshire, UK).

Protein lysate preparation, SDS-PAGE and western blotting

Total protein was extracted from E18.5 skin in sample buffer (125 mM Tris-HCl, pH 6.8, 10% glycerol, 1% SDS). The samples were homogenized using an Ultra-Turrax (Ika, Staufen, Germany) and heated to 95℃ for 5 minutes. Insoluble material was removed by centrifugation. Protein concentration was determined using a BCA kit (Thermo Scientific, Cramlington, UK) according to the manufacturer's instructions. Before the protein lysates were loaded at 10 μg/lane on 8% or 12% polyacrylamide gels and electrophoretically separated using the Laemmli buffer system, β-mercaptoethanol (5% final concentration) and Bromophenol Blue (0.01% final concentration) were added and the samples were heated for 3 minutes at 65℃. After separation, proteins were electrotransferred to a polyvinylidene difluoride (PVDF) membrane (Millipore) using Towbin buffer (25 mM Tris, 192 mM glycine, 10% methanol, pH 8.3). For antigen detection the same primary antibodies were used as for immunofluorescence analysis and the following additional antibodies: anti-K15 (GP15.1, Progen), 1:200; anti-K2 (GP-CK2e, Progen), 1:5000; anti-desmoplakin (DP 495), 1:4000; anti-desmoglein 1 (p124), 1:200; anti-plakoglobin (PG), 1:1000 (the last three were kind gifts from Lutz Langbein, German Cancer Research Center, Heidelberg, Germany); anti-desmocollin (52-3D, David Garrod), 1: 500; GAPDH (6C5, Millipore), diluted 1:300, used as a loading control. Horseradish-peroxidase-conjugated species-specific secondary antibodies (Dianova) were used, and immunodetection was performed using Pierce Super Signal West Pico and Dura substrates (Thermo Scientific).

Barrier function assays

A dye exclusion assay (Hardman et al., 1998) was used on mouse embryos, stage E18.5. Mice were exposed to a methanol series (25, 50, 75 and 100, 75, 50, 25% methanol) for 1 minute each, then washed for 1 minute in PBS and subsequently stained for 5 minutes in 0.2% Toluidine Blue in water. They were then rinsed 3× for 1 minute each in 90% ethanol, washed in water and immediately photographed.

To assess the inside-out barrier function, a tight junction permeability assay (Furuse et al., 2002) was used. 50 μl of 10 mg/ml Pierce EZ-Link Sulfo-NHS-LC-Biotin (Thermo Scientific) in PBS containing 1 mM $CaCl_2$ was injected into the back skin of neonatal mice. After 30 minutes, the injected area of skin was excised and then frozen in isopentane cooled by liquid nitrogen. Cryosections of 5 μm were fixed for 30 minutes at 4℃ in ethanol followed by 1 minute in acetone at ambient temperature. Streptavidin-conjugated Alexa Fluor 594 (Molecular Probes) and an Axio Imager Z2 were used for visualisation.

Cornified envelope analysis

Neonatal skin (approximately 0.5 cm^2) was boiled for 20 minutes in cornified envelope (CE) isolation buffer (20 mM Tris-HCl, pH 7.5; 5 mM EDTA; 10 mM DTT and 2% SDS) according to the method described by Aho et al. (Aho et al., 2004). CEs were centrifuged at 6000 ***g*** and pellets washed with CE washing buffer (CE isolation buffer containing 0.2% SDS), centrifuged as before, and resuspended in washing buffer. CEs were imaged by phase contrast microscopy using a Leica DMJRB microscope equipped with LAS V3.6 software and a DFC-360FX camera.

Electron microscopy

The skin of E18.5 mice was gently dissected, cut into 2 mm^2 pieces using a scalpel and fixed in 2% glutaraldehyde (Agar Scientific) in sodium cacodylate buffer for 4 hours at room temperature and then kept at 4℃ until further processed. Specimens were rinsed 3× for 30 minutes in cacodylate buffer then fixed for 1 hour in 1% osmium tetroxide in cacodylate buffer, and then again rinsed 3× for 30 minutes in cacodylate buffer. Specimens were dehydrated using 25% acetone, 50% acetone and 75% acetone for 30 minutes each; then impregnated with 25% epoxy resin (TAAB Laboratories Equipment, Aldermaston, UK) in acetone, 50% resin in acetone and 75% resin in acetone for 1 hour each and finally with 100% resin changed three times over 24 hours. They were then embedded in 100% resin at 60℃ for 24 hours. Ultrathin sections were cut using a glass knife on an RMC MT-XL ultramicrotome. Sections were stretched with chloroform and mounted on Pioloform-filmed copper grids. Sections were stained with 2% aqueous uranyl acetate and lead citrate (Leica). Sections were examined using a Philips CM 100 Compustage (FEI, Cambridge, UK) transmission electron microscope and digital images were collected using an AMT CCD camera (Deben, Bury St. Edmunds, UK).

Student's *t*-test was used for statistical analysis of desmosome size, and values are given as means ± standard deviation.

Acknowledgements

We thank Prof. Thomas Magin for providing *Krt1*$^{+/-}$ mice, Lutz Langbein, Akis Karakesisoglou and David Garrod for providing antibodies, and Fiona Oakley for her constant support. Furthermore, we thank Rebecca Porter, Birgitte Lane and Rudolf Leube for critically reading the manuscript. For excellent technical assistance and advice with TEM we thank the Electron Microscopy Research Services, and for excellent technical support and advice we thank the Comparative Biology Centre staff, both at Newcastle University.

Funding

This work was supported by the Physiological Society (Travel grant to J.R.); the Ichthyosis Support Group [grant number 09-ISG-002 to J.R. (supported L.R.-T.)]; the Newcastle Health Care Charity and the Newcastle upon Tyne Hospitals NHS Charity [grant number PFC/ML/0809 to J.R.]; the Institute of Cellular Medicine and the Faculty of Medical Sciences of Newcastle University (J.R.).

References

Aho, S., Li, K., Ryoo, Y., McGee, C., Ishida-Yamamoto, A., Uitto, J. and Klement, J. F. (2004). Periplakin gene targeting reveals a constituent of the cornified envelope dispensable for normal mouse development. *Mol. Cell. Biol.* **24**, 6410-6418.

Baribault, H. and Oshima, R. G. (1991). Polarized and functional epithelia can form after the targeted inactivation of both mouse keratin 8 alleles. *J. Cell Biol.* **115**, 1675-1684.

Candi, E., Schmidt, R. and Melino, G. (2005). The cornified envelope: a model of cell death in the skin. *Nat. Rev. Mol. Cell Biol.* **6**, 328-340.

Chamcheu, J. C., Siddiqui, I. A., Syed, D. N., Adhami, V. M., Liovic, M. and Mukhtar, H. (2011). Keratin gene mutations in disorders of human skin and its appendages. *Arch. Biochem. Biophys.* **508**, 123-137.

Chan, Y., Anton-Lamprecht, I., Yu, Q. C., Jackel, A., Zabel, B., Ernst, J. P. and Fuchs, E. (1994). A human keratin 14 "knockout": the absence of K14 leads to severe epidermolysis bullosa simplex and a function for an intermediate filament protein. *Genes Dev.* **8**, 2574-2587.

Crisp, M., Liu, Q., Roux, K., Rattner, J. B., Shanahan, C., Burke, B., Stahl, P. D. and Hodzic, D. (2006). Coupling of the nucleus and cytoplasm: role of the LINC complex. *J. Cell Biol.* **172**, 41-53.

Dahl, K. N. and Kalinowski, A. (2011). Nucleoskeleton mechanics at a glance. *J. Cell Sci.* **124**, 675-678.

Dahl, K. N., Ribeiro, A. J. and Lammerding, J. (2008). Nuclear shape, mechanics, and mechanotransduction. *Circ. Res.* **102**, 1307-1318.

Furuse, M., Hata, M., Furuse, K., Yoshida, Y., Haratake, A., Sugitani, Y., Noda, T., Kubo, A. and Tsukita, S. (2002). Claudin-based tight junctions are crucial for the mammalian epidermal barrier: a lesson from claudin-1-deficient mice. *J. Cell Biol.* **156**, 1099-1111.

Gan, S. Q., McBride, O. W., Idler, W. W., Markova, N. and Steinert, P. M. (1990). Organization, structure, and polymorphisms of the human profilaggrin gene. *Biochemistry* **29**, 9432-9440.

Garrod, D. and Chidgey, M. (2008). Desmosome structure, composition and function. *Biochim. Biophys. Acta* **1778**, 572-587.

Godsel, L. M., Hsieh, S. N., Amargo, E. V., Bass, A. E., Pascoe-McGillicuddy, L. T., Huen, A. C., Thorne, M. E., Gaudry, C. A., Park, J. K., Myung, K. et al. (2005). Desmoplakin assembly dynamics in four dimensions: multiple phases differentially regulated by intermediate filaments and actin. *J. Cell Biol.* **171**, 1045-1059.

Hardman, M. J., Sisi, P., Banbury, D. N. and Byrne, C. (1998). Patterned acquisition of skin barrier function during development. *Development* **125**, 1541-1552.

Herrmann, H., Strelkov, S. V., Burkhard, P. and Aebi, U. (2009). Intermediate filaments: primary determinants of cell architecture and plasticity. *J. Clin. Invest.* **119**, 1772-1783.

Kartasova, T., Roop, D. R., Holbrook, K. A. and Yuspa, S. H. (1993). Mouse differentiation-specific keratins 1 and 10 require a preexisting keratin scaffold to form a filament network. *J. Cell Biol.* **120**, 1251-1261.

Ketema, M., Wilhelmsen, K., Kuikman, I., Janssen, H., Hodzic, D. and Sonnenberg, A. (2007). Requirements for the localization of nesprin-3 at the nuclear envelope and its interaction with plectin. *J. Cell Sci.* **120**, 3384-3394.

Kirfel, J., Magin, T. M. and Reichelt, J. (2003). Keratins: a structural scaffold with emerging functions. *Cell. Mol. Life Sci.* **60**, 56-71.

Koch, P. J., de Viragh, P. A., Scharer, E., Bundman, D., Longley, M. A., Bickenbach, J., Kawachi, Y., Suga, Y., Zhou, Z., Huber, M. et al. (2000). Lessons from loricrin-deficient mice: compensatory mechanisms maintaining skin barrier function in the absence of a major cornified envelope protein. *J. Cell Biol.* **151**, 389-400.

Leclerc, E. A., Huchenq, A., Mattiuzzo, N. R., Metzger, D., Chambon, P., Ghyselinck, N. B., Serre, G., Jonca, N. and Guerrin, M. (2009). Corneodesmosin gene ablation induces lethal skin-barrier disruption and hair-follicle degeneration related to desmosome dysfunction. *J. Cell Sci.* **122**, 2699-2709.

Lin, F., Morrison, J. M., Wu, W. and Worman, H. J. (2005). MAN1, an integral protein of the inner nuclear membrane, binds Smad2 and Smad3 and antagonizes transforming growth factor-beta signaling. *Hum. Mol. Genet.* **14**, 437-445.

Lloyd, C., Yu, Q. C., Cheng, J., Turksen, K., Degenstein, L., Hutton, E. and Fuchs, E. (1995). The basal keratin network of stratified squamous epithelia: defining K15 function in the absence of K14. *J. Cell Biol.* **129**, 1329-1344.

Magin, T. M., Schroder, R., Leitgeb, S., Wanninger, F., Zatloukal, K., Grund, C. and Melton, D. W. (1998). Lessons from keratin 18 knockout mice: formation of novel keratin filaments, secondary loss of keratin 7 and accumulation of liver-specific keratin 8-positive aggregates. *J. Cell Biol.* **140**, 1441-1451.

Magin, T. M., Hesse, M., Meier-Bornheim, R. and Reichelt, J. (2004). Developing mouse models to study intermediate filament function. *Methods Cell Biol.* **78**, 65-94.

Mejat, A., Decostre, V., Li, J., Renou, L., Kesari, A., Hantai, D., Stewart, C. L., Xiao, X., Hoffman, E., Bonne, G. et al. (2009). Lamin A/C-mediated neuromuscular junction defects in Emery-Dreifuss muscular dystrophy. *J. Cell Biol.* **184**, 31-44.

Milner, D. J., Weitzer, G., Tran, D., Bradley, A. and Capetanaki, Y. (1996). Disruption of muscle architecture and myocardial degeneration in mice lacking desmin. *J. Cell Biol.* **134**, 1255-1270.

Moll, R., Divo, M. and Langbein, L. (2008). The human keratins: biology and pathology. *Histochem. Cell Biol.* **129**, 705-733.

Peters, B., Kirfel, J., Bussow, H., Vidal, M. and Magin, T. M. (2001). Complete cytolysis and neonatal lethality in keratin 5 knockout mice reveal its fundamental role in skin integrity and in epidermolysis bullosa simplex. *Mol. Biol. Cell* **12**, 1775-1789.

Postel, R., Ketema, M., Kuikman, I., de Pereda, J. M. and Sonnenberg, A. (2010). Nesprin-3 augments peripheral nuclear localization of intermediate filaments in zebrafish. *J. Cell Sci.* **124**, 755-764.

Presland, R. B., Kuechle, M. K., Lewis, S. P., Fleckman, P. and Dale, B. A. (2001). Regulated expression of human filaggrin in keratinocytes results in cytoskeletal disruption, loss of cell-cell adhesion, and cell cycle arrest. *Exp. Cell Res.* **270**, 199-213.

Razafsky, D. and Hodzic, D. (2009). Bringing KASH under the SUN: the many faces of nucleo-cytoskeletal connections. *J. Cell Biol.* **186**, 461-472.

Reichelt, J. and Magin, T. M. (2002). Hyperproliferation, induction of c-Myc and 14-3-3sigma, but no cell fragility in keratin-10-null mice. *J. Cell Sci.* **115**, 2639-2650.

Reichelt, J., Bauer, C., Porter, R., Lane, E. and Magin, T. M. (1997). Out of balance: consequences of a partial keratin 10 knockout. *J. Cell Sci.* **110**, 2175-2186.

Reichelt, J., Doering, T., Schnetz, E., Fartasch, M., Sandhoff, K. and Magin, T. M. (1999). Normal ultrastructure, but altered stratum corneum lipid and protein composition in a mouse model for epidermolytic hyperkeratosis. *J. Invest. Dermatol.* **113**, 329-334.

Reichelt, J., Bussow, H., Grund, C. and Magin, T. M. (2001). Formation of a normal epidermis supported by increased stability of keratins 5 and 14 in keratin 10 null mice. *Mol. Biol. Cell* **12**, 1557-1568.

Rentrop, M., Nischt, R., Knapp, B., Schweizer, J. and Winter, H. (1987). An unusual type-II 70-kilodalton keratin protein of mouse epidermis exhibiting postnatal body-site specificity and sensitivity to hyperproliferation. *Differentiation* **34**, 189-200.

Schneider, M., Lu, W., Neumann, S., Brachner, A., Gotzmann, J., Noegel, A. A. and Karakesisoglou, I. (2011). Molecular mechanisms of centrosome and cytoskeleton anchorage at the nuclear envelope. *Cell. Mol. Life Sci.* **68**, 1593-1610.

Sevilla, L. M., Nachat, R., Groot, K. R., Klement, J. F., Uitto, J., Djian, P., Maatta, A. and Watt, F. M. (2007). Mice deficient in involucrin, envoplakin, and periplakin have a defective epidermal barrier. *J. Cell Biol.* **179**, 1599-1612.

Stewart, C. L., Roux, K. J. and Burke, B. (2007). Blurring the boundary: the nuclear envelope extends its reach. *Science* **318**, 1408-1412.

Vasioukhin, V., Bowers, E., Bauer, C., Degenstein, L. and Fuchs, E. (2001). Desmoplakin is essential in epidermal sheet formation. *Nat. Cell Biol.* **3**, 1076-1085.

Vijayaraj, P., Sohl, G. and Magin, T. M. (2007). Keratin transgenic and knockout mice: functional analysis and validation of disease-causing mutations. *Methods Mol. Biol.* **360**, 203-251.

Wilhelmsen, K., Litjens, S. H., Kuikman, I., Tshimbalanga, N., Janssen, H., van den Bout, I., Raymond, K. and Sonnenberg, A. (2005). Nesprin-3, a novel outer nuclear membrane protein, associates with the cytoskeletal linker protein plectin. *J. Cell Biol.* **171**, 799-810.